Check for updates

Received: 19 October 2023 | Revised: 12 February 2024 | Accepted: 20 February 2024

DOI: 10.1002/oby.24023

ORIGINAL ARTICLE

Obesity Biology and Integrated Physiology

Obesity A Research Journal | THE OBESITY SOCIETY | WILEY

Human epicardial fat has a beige profile and contains higher type 2 innate lymphoid cells than subcutaneous fat

Elisa Doukbi[1] | Patricia Ancel[1] | Anne Dutour[1,2] | Astrid Soghomonian[1,2] | Shaista Ahmed[1,3] | Victoria Castejon[1] | Christelle Piperoglou[4] | Vlad Gariboldi[1,5] | Marien Lenoir[6] | Eric Lechevallier[7] | Bastien Gondran-Tellier[7] | Romain Boissier[7] | Mikael Ebbo[4,8] | Frédéric Vély[4] | Bénédicte Gaborit[1,2]

[1]Aix-Marseille University, National Institute for Health and Medical Research (INSERM), National Research Institute for Agriculture, Food and the Environment (INRAE), Cardiovascular and Nutrition Research Center (C2VN), Marseille, France

[2]Department of Endocrinology, Metabolic Diseases and Nutrition, Pole Endocrinology-Nutrition-Diabetes-Obesity, Public Assistance Marseille Hospitals, Marseille, France

[3]Heart Repair and Regeneration Laboratory, Department of Endocrinology, Metabolism, and Cardiovascular System, Faculty of Sciences and Medicine, University of Fribourg, Fribourg, Switzerland

[4]Aix-Marseille University, CNRS, National Institute for Health and Medical Research (INSERM), Marseille-Luminy Immunology Center (CIML), Marseille University Hospital Timone, Public Assistance Marseille Hospitals, Marseille Immunopole, Marseille, France

[5]Department of Cardiac Surgery, Marseille University Hospital Timone, Public Assistance Marseille Hospitals, Marseille, France

[6]Division of Paediatric Cardiac Surgery, Marseille University Hospital Timone, Public Assistance Marseille Hospitals, Marseille, France

[7]Department of Urology Surgery, Conception Hospital, Public Assistance Marseille Hospitals, Marseille, France

[8]Internal Medicine Department, Marseille University Hospital Timone, Public Assistance Marseille Hospitals, Marseille, France

Correspondence
Bénédicte Gaborit, Faculty of Medical and Paramedical Sciences, C2VN, 27 Boulevard Jean Moulin, 13005 Marseille, France.
Email: benedicte.gaborit@univ-amu.fr

Abstract

Objective: Epicardial adipose tissue (EAT) is a visceral fat that has been associated with coronary artery disease and atrial fibrillation. Previous work has revealed that EAT exhibits beige features.

Methods: First, a new pan-genomic microarray analysis was performed on previously collected paired human EAT and thoracic subcutaneous AT (thSAT) from the EPICAR study ($n = 31$) to decipher a specific immune signature and its link with browning genes. Then, adaptive (T and B cells) and innate lymphoid cell (ILC1, ILC2, and ILC3) immunophenotyping assay panels, including CD127, CD117, and prostaglandin D2 receptor 2, were performed on prospectively collected paired human multiorgan donors ($n = 18$; INTERFACE study).

Results: In the EPICAR study, a positive correlation between the T helper cell subtype Th2 immune pathway and browning genes was found in EAT versus thSAT ($r = 0.82$; $p < 0.0001$). In the INTERFACE study, this correlation was also observed ($r = 0.31$; $p = 0.017$), and a preponderance of $CD4^+$T cells, $CD8^+$T cells, and a few B cells was observed in all ATs ($p < 0.0001$). An increase in ILCs was observed in visceral AT (VAT) (i.e., EAT + VAT; 30 ± 5 ILCs per gram of AT) compared with subcutaneous counterparts (i.e., thSAT + abdominal SAT; 8 ± 2 ILCs per gram of AT; $p = 0.001$), with ILC1 being the most frequent (ILC1 > ILC3 > ILC2). Numbers of ILCs per gram of AT correlated with several Th2 or browning genes (IL-13, TNF receptor superfamily member 9 [TNFRSF9], and alkaline phosphatase, biomineralization associated [ALPL]). Interestingly, a specific increase in EAT-ILC2 compared with other ATs was observed, including a significant proportion expressing CD69 and/or CD25 activation markers (97.9% ± 1.2%; $p < 0.0001$). Finally, more natural killer cells were observed in EAT + VAT than in thSAT + abdominal SAT ($p = 0.01$). Exclusion of patients with coronary artery disease in the EPICAR and INTERFACE studies did not modify the main findings. Gene

See Commentary, pg. X.

This is an open access article under the terms of the Creative Commons Attribution-NonCommercial License, which permits use, distribution and reproduction in any medium, provided the original work is properly cited and is not used for commercial purposes.
© 2024 The Authors. *Obesity* published by Wiley Periodicals LLC on behalf of The Obesity Society.

Funding information
Aix-Marseille University Excellence Initiative—A*MIDEX, Grant/Award Number: AMX-21-PEP-026; Fondation de l'Avenir, Grant/Award Number: AP-RM-22-017

expression phenotyping confirmed specific upregulation of Th2 pathway and browning genes (IL-33 and uncoupling protein 1 [UCP-1]) in EAT.

Conclusions: This is the first study, to our knowledge, to provide a comparison between innate and adaptive lymphoid cells in human EAT. Further studies are ongoing to decipher whether these cells could be involved in EAT beiging.

INTRODUCTION

Epicardial adipose tissue (EAT) is, in the human heart, the unique visceral AT (VAT) that is in direct contact with the myocardium and coronary arteries. The emerging role of this ectopic AT in cardiovascular diseases has led to a growing interest. Nowadays, EAT is increasingly recognized as an endocrine organ capable of secreting adipokines that can have a direct impact on the metabolism of the heart and coronary arteries [1, 2]. Although EAT secretome can have physiologically positive effects (adiponectin), it can also represent a source of proinflammatory (C-C motif chemokine ligand 2 [CCL2], interleukin [IL]-6, tumor necrosis factor α [TNFα], chemerin, resistin, and serglycin) or profibrotic molecules (activin-A and transforming growth factor β) that could exert adverse effects on the heart and coronary arteries [3]. EAT is believed to be a direct source of heat for the myocardium and protects the heart from unfavorable hemodynamic conditions such as ischemia, hypothermia, or hypoxia. However, the imbalance between protective and deleterious EAT adipokines may also participate in the proinflammatory phenotype associated with endothelial dysfunction and atherogenesis [4, 5]. In the past few years, its secretome was shown to switch into a proinflammatory profile in obesity and coronary artery disease (CAD) inducing atherogenic changes in monocytes [6, 7]. Elucidating factors implicated in the balance between the pro- and anti-inflammatory immune cells seem to be a key element in atherogenesis and could represent a future therapeutic target. The innate lymphoid cell (ILC) family is composed of natural killer (NK) cytotoxic cells and helper cells, i.e., ILC1, ILC2, and ILC3, which are mostly tissue-resident and could participate in regulating AT inflammation or homeostasis. Using transcriptomic studies, we and others have shown that EAT exhibits a brown fat-like or beige phenotype [8, 9], with a high expression of thermogenic genes such as uncoupling protein (UCP)-1 or peroxisome proliferator activated receptor γ (PPARγ) coactivator 1 α (PPARGC1A) and a specific lipidomic plasmalogen enrichment that could reflect a specific thermogenic activity [9, 10]. Remarkably, recent studies have demonstrated that ILC2, the innate counterparts of T helper subtype Th2 cells, are critically involved in the browning of AT [11, 12]. Indeed, ILC2 have been shown to activate a thermogenic circuit that directly promotes the expansion and commitment of beige adipocyte progenitors in subcutaneous AT (SAT) [13]. ILC1 are another subclass of ILCs that can contribute to AT inflammation. In diet-induced obesity, ILC1-derived interferon (IFN)-γ was necessary and sufficient to drive proinflammatory macrophage polarization and to promote obesity-associated insulin resistance [14]. In this study, we aimed at prospectively analyzing the

Study Importance

What is already known?

- Epicardial adipose tissue (EAT) is a biologically active ectopic fat depot surrounding the myocardium and coronary arteries. Its abundance has been implicated in cardiovascular diseases such as atrial fibrillation and coronary artery disease.
- Our group has demonstrated that EAT exhibits a beige phenotype.
- Immune cells can be involved in the AT beiging/browning phenomenon. In rodents, innate lymphoid cells (ILCs), particularly type 2 (i.e., ILC2), have been found to induce beiging and type 1 (i.e., ILC1) inflammation, but their presence has never been studied in human EAT, to our knowledge.

What does this study add?

- This study is the first, to our knowledge, to describe individual immune cell populations and identify ILCs in human EAT using multiparametric flow cytometry methods.
- An increase in T cells compared with B cells was evidenced in all ATs, and an increase in ILCs (ILC1 > ILC3 > ILC2) and natural killer cells was observed in visceral versus subcutaneous AT.
- Remarkably, a specific enrichment of ILC2 in EAT was observed compared with other ATs, and these ILC2 were found to be highly activated.

How might these results change the direction of research or the focus of clinical practice?

- These new preliminary findings could suggest that ILC1/ILC2 might play a role in the inflammation/beiging profile of EAT.
- The cellular players and molecular targets responsible for this specific EAT phenotype have yet to be discovered and could represent future therapeutic targets to prevent coronary artery disease.

1930739x, 0, Downloaded from https://onlinelibrary.wiley.com/doi/10.1002/oby.24023 by Cochrane France, Wiley Online Library on [16/05/2024]. See the Terms and Conditions (https://onlinelibrary.wiley.com/terms-and-conditions) on Wiley Online Library for rules of use; OA articles are governed by the applicable Creative Commons License

presence of adaptive lymphoid cells and ILCs in the human EAT stromal vascular fraction (SVF) compared with abdominal VAT and thoracic and abdominal SAT (thSAT and abSAT, respectively).

METHODS

Patients and collection of samples

First retrospective cohort: the EPICAR study

A new pan-genomic microarray analysis was performed on a previous transcriptomic dataset obtained from the EPICAR study, including 118 biopsies of 31 paired thSAT and EAT samples [9], to identify a specific immune signature and its link with browning genes. This transcriptomic study was approved by the local ethics committee of Pitié-Salpêtrière Hospital (Paris, France) and North Hospital (Marseille, France). This study was performed in accordance with the Declaration of Helsinki. All patients signed their written informed consent. The aim of the EPICAR study was to identify the transcriptomic signature of EAT collected from different anatomical regions (atrial, pericoronary, and periventricular EAT). In this new study, we reused pan-genomic data from all of our EAT samples and tried to decipher whether the EAT browning profile was related to the Th2 cell pathway.

Second prospective cohort: the INTERFACE study

Prospective paired EAT, VAT, thSAT, and abSAT biopsies from brain dead multiorgan donors ($n = 18$) were then collected for flow cytometry (FC) analyses and identification of AT immune cell populations. A minimum of 20 mg of each AT was necessary to perform FC analyses. All of the donors' families gave their signed written informed consent for the scientific sampling protocol. This protocol was approved by the National Ethics Committee of the French Biomedicine Agency (registration number PFS21-005), and collection was declared to the Ministry of Higher Education, Research, and Innovation (CODECOH N° DC-2021-4518) and adhered to the Jardé Law on human investigation. Absence of objection from the deceased donors' families was systematically verified by the organ donation coordination team.

Transcriptomic study

RNA was extracted and analyzed through a pan-genomic approach using HumanHT-12 version 4 Illumina BeadChip containing 47,231 probes for 28,688 coded transcripts. A quantile normalization was used to eliminate bad quality signals. Principal components analysis, partial least-squares discriminant analysis, and gene score calculation were performed with SIMCA (Sartorius AG) and Prism (GraphPad Software). The score was obtained from contribution of separate orthogonal partial least-squares discriminant analyses calculated from Th2 cells or browning sets of genes (genes with variable importance in the projection [VIP] value > 0.8), allowing for each set to generate a composite score value. The following browning gene set was selected from peer literature review [12, 15]: UCP-1; UCP-2; UCP-3; TNF receptor superfamily member 9 (TNFRSF9); adrenoceptor β 3 (ADRB3); PPARGC1A; PR/SET domain 16 (PRDM16); activating transcription factor 2 (ATF2); zinc finger CCCH-type containing 10 (ZC3H10); nuclear respiratory factor 1 (NRF1); transcription factor A, mitochondrial (TFAM); CD81 molecule (CD81); Cbp/p300 interacting transactivator with Glu/Asp rich carboxy-terminal domain 1 (CITED1); epithelial stromal interaction 1 (EPSTI1); fatty acid binding protein 1 (FABP4); SHOX homeobox 2 (SHOX2); solute carrier family 2 member 4 (SLC2A4); T-box transcription factor 1 (TBX1); bone morphogenetic protein 7 (BMP7); cell death inducing DFFA like effector A (CIDEA); carnitine palmitoyltransferase 1b (CPT1B); EBF transcription factor 2 (EBF2); NADH:ubiquinone oxidoreductase subunit B6 (NDUFB6); sirtuin 5 (SIRT5); translocase of inner mitochondrial membrane 23 (TIMM23); and transmembrane protein 26 (TMEM26). The following Th2 cell gene set was also selected from peer literature review [12, 15]: IL-2; IL-4; IL-5; IL-9; IL-13; IL-25; IL-33; thymic stromal lymphopoietin (TSLP); colony stimulating factor 2 (CSF2); amphiregulin (AREG); killer cell lectin-like receptor G1 (KLRG1); inducible T cell costimulator (ICOS); GATA binding protein 3 (GATA3); sperm-associated antigen 5 (SPAG5); cyclin B1 (CCNB1); RAD51-associated protein 1 (RAD51AP1); hyaluronan-mediated motility receptor (HMMR); denticleless E3 ubiquitin protein ligase homolog (DTL); SHC binding and spindle associated 1 (SHCBP1); thymidine kinase 1 (TK1); BUB1 mitotic checkpoint serine/threonine kinase B (BUB1B); ribonucleotide reductase regulatory subunit M2 (RRM2); kinesin family member 23 (KIF23); baculoviral IAP repeat containing 5 (BIRC5); minichromosome maintenance complex component 6 (MCM6); TTK protein kinase (TTK); maternal embryonic leucine zipper kinase (MELK); and ubiquitin-like with PHD and ring finger domains 1 (UHRF1). Th2 cell aggregation of the data into a gene score block enables an ease of data interpretation with a correlation analysis. The difference in gene expression between thSAT and EAT was performed with significant analysis of microarray (SAM) analysis, which provides a list of significant genes (VIP > 0.8) and false discovery rate (FDR). Pathway enrichment was analyzed with Ingenuity Pathway Analysis (IPA; QIAGEN) using canonical ingenuity pathway database.

Prospective AT SVF extraction

SVF from the collected AT was obtained by mechanical and enzymatic dissociation, as previously described [16, 17]. Briefly, AT was cut into small pieces and then dissociated with 0.5-mg/mL collagenase A (Roche) for 30 to 45 min at 37°C under agitation. The dissociation products were then filtered and centrifuged for 5 min at 550*g* at room temperature. SVF was then incubated with 1 mL of red blood cell lysis buffer (115mM ammonium chloride [NH_4Cl], 10mM potassium bicarbonate [$KHCO_3$], and 0.1mM EDTA) for 10 min at room temperature with gentle agitation and centrifuged for 5 min at 550*g* at room temperature. The pellet was then washed in 5 mL of buffer (0.1mM EDTA-phosphate-buffered saline [PBS], Gibco, Thermo Fisher Scientific) and filtered on 100-µm nylon filter (BD Falcon). Filtrate was then

1930739x, 0, Downloaded from https://onlinelibrary.wiley.com/doi/10.1002/oby.24023 by Cochrane France, Wiley Online Library on [16/05/2024]. See the Terms and Conditions (https://onlinelibrary.wiley.com/terms-and-conditions) on Wiley Online Library for rules of use; OA articles are governed by the applicable Creative Commons License

centrifuged for 5 min at 300*g* at room temperature, and the pellet was suspended in fluorescence activated cell sorting (FACS) buffer (bovine serum albumin [BSA] 1%, EDTA 2mM-PBS) prior to FC.

Prospective FC

Two sets of FC analyses were performed, as previously described [18, 19]. First, lymphocyte populations were analyzed. To this end, total lymphocytes, $CD3^+$T cells, $CD4^+$T cells, $CD8^+$T cells, $CD19^+$B cells, and $CD3^+CD56^+$ NK cells were quantified using BD Multitest 6-color and BD Trucount technologies. Fifty microliters of samples was incubated for 15 min in the dark at room temperature before addition of BD lysis buffer. Cells were gated on CD45 (hematopoietic cells) and respectively stained with CD3 (T cells), CD4 ($CD4^+$T cells), CD8 ($CD8^+$T cells), CD19 (B cells), and CD16/CD56 (NK cells) antibodies. Samples were analyzed on a BD FACSCanto II cytometer using the BD FACSCanto software.

Secondly, a peripheral blood mononuclear cell panel was used to characterize ILCs by FC [18, 19]. SVF cells were centrifuged for 5 min at 4°C and 645*g*. Then, they were incubated with 5 µL of BD Fc Block at room temperature for 10 min. Samples were then mixed with a fluorescein isothiocyanate (FITC) exclusion lineage antibody panel (T cell receptor [TCR]γδ, TCRαβ, CD3, CD19, CD14, CD16, CD94, CD123, CD34, CD303, and FcεRI) and 50 µL of BD Horizon Brilliant Stain Buffer before adding specific antibodies (CD45, CD127, CD7, CD56, CD161, CD117, prostaglandin D2 receptor 2 [CRTH2], CD5, CCR6, CD69, CD25, NKp44, and NKp46). The mix was incubated for 30 min at room temperature and in obscurity. We thereby used cell-surface expression of CD127, CD117, and CRTH2 to identify ILC1, ILC2, and ILC3 subsets, respectively, defined as $Lin^-CD127^+CD117^-CRTH2^-$ cells, $Lin^-CD127^+CRTH2^+$ cells, and $Lin^-CD127^+CD117^+$ $CRTH2^-$ cells. These data were acquired with a BD LSRFortessa X-20 cytometer and were analyzed on FlowJo version 10.8.1 software.

RNA extraction/reverse transcription-quantitative polymerase chain reaction (INTERFACE study)

RNA was extracted using the PureLink RNA Mini Kit (Life Technologies), and total RNA concentration was measured by the use of a BioDrop spectrophotometer (Biochrom Ltd). Reverse transcription-quantitative polymerase chain reaction (RT-qPCR) was performed with 100 ng of RNA, 20 U/µL of SuperScript II RT (Life Technologies), 200 ng/µL of random primers, 10mM nucleotides, and 40 U/µL of the ribonuclease inhibitor RNaseOUT (Life Technologies). Primers for qPCR (Table S1) were designed via OligoArchitect (Sigma-Aldrich). qPCR was performed using primers labeled with fluorescent EvaGreen (Euromedex) and a real-time thermocycler, i.e, LightCycler 480 (Roche). The ribosomal protein lateral stalk subunit P0 (RPLP0) ribosomal gene was used as reference gene to normalize cycle thresholds (Ct) and to obtain relative quantification (ΔΔCt) [20].

Statistics

For transcriptomic analyses (EPICAR and INTERFACE studies), correlation between Th2 cells and browning gene expression scores was analyzed using Spearman rank correlation coefficient. For multiblock analyses, the level of significance used was FDR < 0.05. In the prospective INTERFACE study, FC data from paired EAT, VAT, thSAT, and abSAT were all first analyzed separately. Then, because EAT and VAT are both VAT when thSAT and abSAT are both SAT, their data were pooled to analyze paired VAT (EAT + VAT) and SAT (thSAT + abSAT). Data are shown as mean ± SEM and box plot data with the Tukey method ($p < 0.05$ considered as statistically significant). For the prospective analysis (INTERFACE study), the differences in gene expression quantified by RT-qPCR were analyzed using the Kruskal–Wallis test and, as appropriate, Dunn post hoc test. Correlation between ILCs per gram of AT and relative gene expression was analyzed using Spearman nonparametric test. The level of significance used was $p < 0.05$. Statistical analyses were performed using Prism version 10 (GraphPad Software).

RESULTS

Patient characteristics

Retrospective transcriptomic study

Pan-genomic microarray analysis was performed on 31 patients who had an average age of 67.3 ± 10.4 years [9]. This population had an average body mass index (BMI) of 28.0 ± 4.5 kg/m^2; 54% of them had CAD; 63% had hypertension; 54% had dyslipidemia; 29% had type 2 diabetes (T2D); and 49% of them smoked, as previously described [9].

Prospective FC study

A total of 18 multiorgan donor patients were included in this study. These patients had an average age of 56 ± 16 years; average BMI of 27.2 ± 4.2 kg/m^2; 6% had CAD; 44% had hypertension; 17% had dyslipidemia; 2% had obesity; 6% had T2D; and 50% had a history of smoking (Table 1).

Epicardial fat is enriched in Th2 cell signaling pathway transcripts that also correlate with browning genes

Transcriptomic analysis revealed an average of 9700 ± 105 detected genes (Figure 1A). Principal components analysis on SIMCA showed that EAT depots clustered differently from thSAT (Figure 1B). Moreover, SAM analysis significantly identified 2123 upregulated genes and 1813 downregulated genes in EAT compared with thSAT (FDR < 0.05). The significant genes with VIP >0.8 were IL-4, IL-5, IL-9, IL-13, IL-25, IL-33, KLRG1, HMMR, BUB1B, KIF23, MCM6, UHRF1, and MELK for Th2 cell score and UCP-1, PPARGC1A, PRDM16, NRF1, CD81, EPSTI1, FABP4,

1930739x, 0, Downloaded from https://onlinelibrary.wiley.com/doi/10.1002/oby.24023 by Cochrane France, Wiley Online Library on [16/05/2024]. See the Terms and Conditions (https://onlinelibrary.wiley.com/terms-and-conditions) on Wiley Online Library for rules of use; OA articles are governed by the applicable Creative Commons License

TABLE 1 Clinical characteristics of multiorgan donor patients ($n = 18$)

	Multiorgan donor population
Patients (F/M)	18 (6/12)
Age (y)	56 ± 16
BMI (kg/m^2)	27.2 ± 4.2
Obesity, BMI ≥ 30 kg/m^2	2 (11%)
Waist circumference (cm)	98 ± 14
F	97 ± 15
M	95 ± 12
T2D	1 (6%)
Hypertension	8 (44%)
Smoking history, ever	9 (50%)
Dyslipidemia	3 (17%)
CAD	1 (6%)

Note: Data shown as mean ± SD or *n* (%).
Abbreviations: CAD, coronary artery disease; F, female; M, male; T2D, type 2 diabetes.

SHOX2, SLC2A4, and TMEM26 for browning score. Interestingly, functional analysis of genes using IPA showed that EAT-enriched pathways were related to Th2 cell immune response (IL-4 and IL-13 signaling) and browning, including mitochondrial dysfunction, oxidative phosphorylation, and white AT browning ($r = 0.82$; $p < 0.0001$; Figure 1C,D). The exclusion of patients with CAD did not alter the relationship between Th2 cells and browning score in EAT (Figure S1). In the INTERFACE prospective study, we confirmed significant consistent correlation between Th2 cells and browning genes ($r = 0.31$; $p = 0.017$; data not shown).

All ATs have the same adaptive cell distribution tendency

FC analyses revealed a significantly higher proportion of T cells (18,886 ± 23,313 cells per gram of tissue) compared with B cells (447 ± 955 cells per gram of tissue; $p < 0.0001$) in all ATs (Figure 2A). In addition, CD4$^+$T cells were more represented than their cytotoxic counterpart CD8$^+$T cells (Figure 2A). No significant difference was found in the amount of adaptive lymphoid cells among ATs

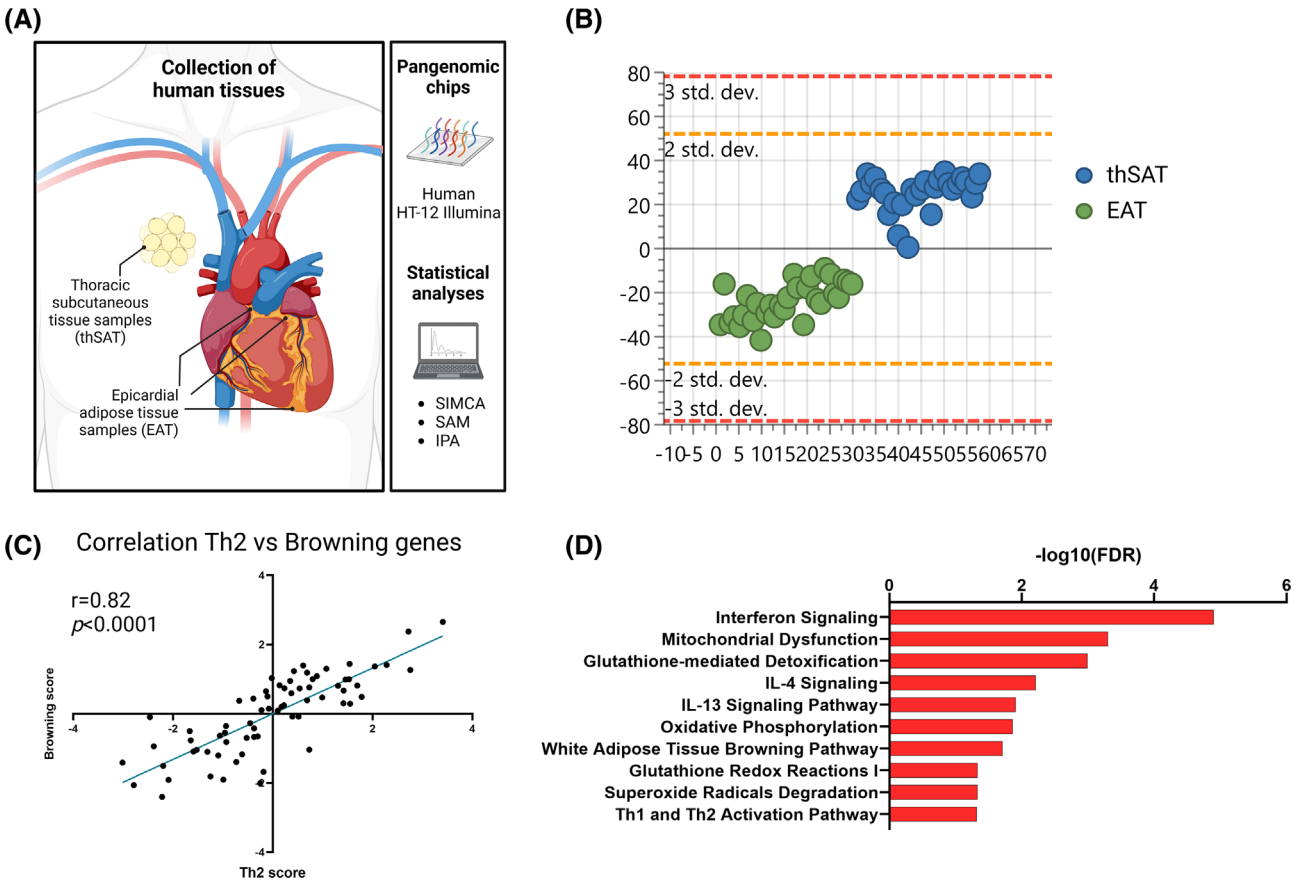

FIGURE 1 Relationship between Th2 cell pathway and browning genes in epicardial adipose tissue (EAT) compared with thoracic subcutaneous AT (thSAT) using significant analysis of microarray (SAM), SIMCA, and Ingenuity Pathway Analysis (IPA) in the EPICAR study. (A) Site collection of AT. (B) Principal components analysis including EAT and thSAT genes. (C) Correlation between Th2 and browning scores in EAT. (D) IPA showing the most important pathways associated with EAT compared with thSAT. The variable importance in the projection value (VIP) was selected as >0.8; Th2 gene set is as follows: IL-4, IL-5, IL-9, IL-13, IL-25, IL-33, KLRG1, HMMR, UHRF1, BUB1B, KIF23, MELK, MCM6; Browning gene set: UCP1, PPARGC1A, PRDM16, NRF1, CD81, EPSTI1, FABP4, SHOX2, SLC2A4, and TMEM26. [Color figure can be viewed at wileyonlinelibrary.com]

1930739x, 0, Downloaded from https://onlinelibrary.wiley.com/doi/10.1002/oby.24023 by Cochrane France, Wiley Online Library on [16/05/2024]. See the Terms and Conditions (https://onlinelibrary.wiley.com/terms-and-conditions) on Wiley Online Library for rules of use; OA articles are governed by the applicable Creative Commons License

(Figure S2A–D). On the other hand, VAT (EAT + VAT) contained significantly more $CD3^+$ cells ($p < 0.05$) as well as $CD4^+$T cells ($p < 0.05$) and $CD8^+$T cells ($p < 0.05$) than SAT (thSAT + abSAT), but there was no significant difference for B cell distribution ($p = 0.35$; Figure S2E–H). Together, these results show that EAT, VAT, thSAT, and abSAT have the same tendency of adaptive immune cell

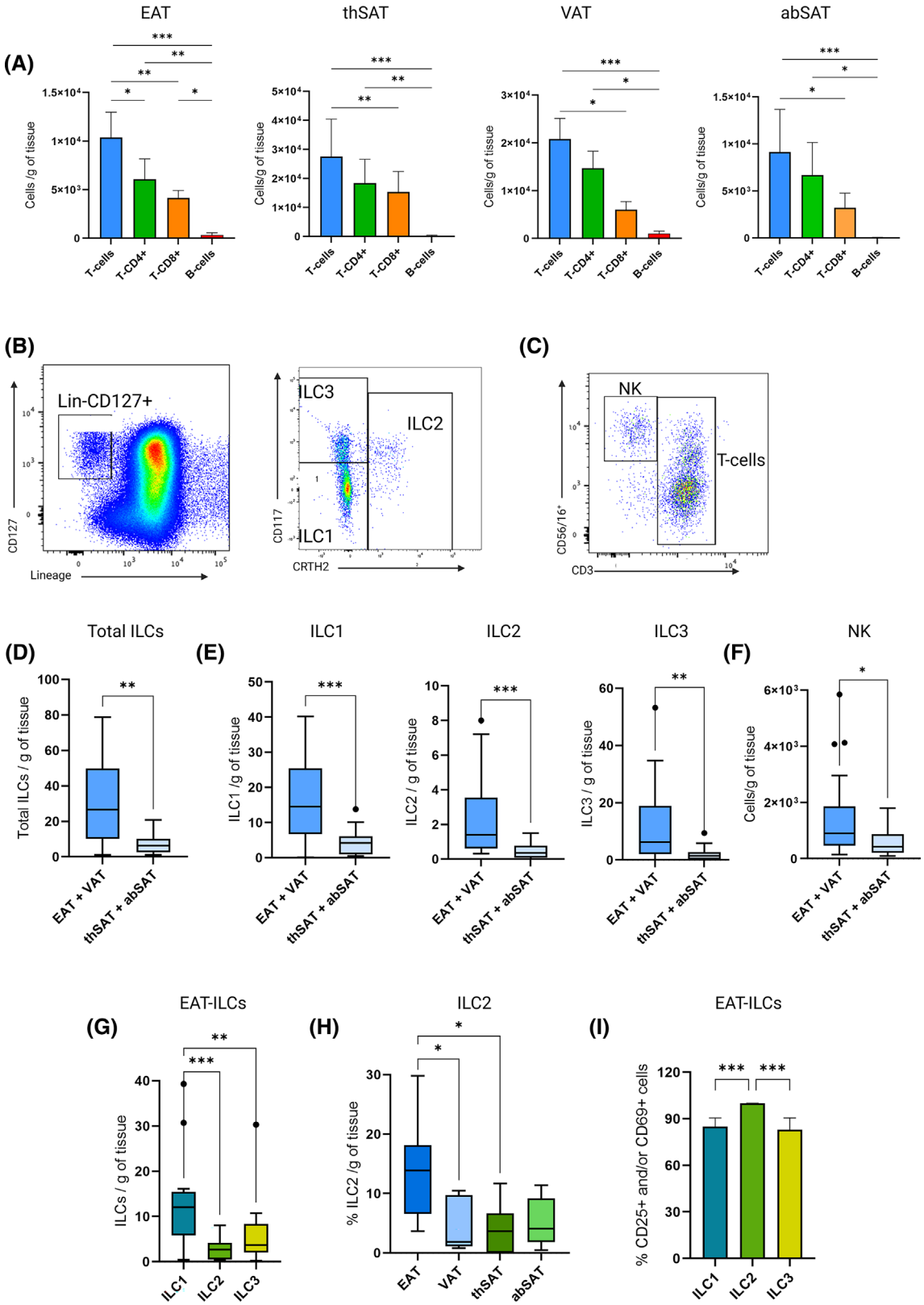

FIGURE 2 Legend on next page.

1930739x, 0, Downloaded from https://onlinelibrary.wiley.com/doi/10.1002/oby.24023 by Cochrane France, Wiley Online Library on [16/05/2024]. See the Terms and Conditions (https://onlinelibrary.wiley.com/terms-and-conditions) on Wiley Online Library for rules of use; OA articles are governed by the applicable Creative Commons License

proportions and that VAT contains more adaptive immune cells than SAT. Exclusion of a patient with CAD did not significantly change the results (Figure S3).

VAT contains more ILCs than SAT

We next performed multiparametric FC assay to identify AT ILCs and NK cells (Figure 2B,C). VAT showed a significant increase in ILC1 and ILC3 compared with thSAT ($p < 0.05$; Figure S4). Interestingly, the total number and the number of ILCs per gram from AT were significantly increased in VAT (EAT + VAT) compared with SAT (EAT + VAT: 30 ± 5 ILCs per gram of AT; thSAT + abSAT: 8 ± 2 ILCs per gram of AT; $p = 0.001$), and this was also observed for each ILC subset (Figure 2D,E). We also observed more NK cells in EAT and VAT (2208 ± 843 cells per gram of AT) than in SAT (586 ± 127 cells per gram of AT; $p = 0.01$; Figure 2F). Interestingly, there was a difference in the proportion of the three subtypes of ILCs (62% ± 3% of ILC1 vs. 24% ± 3% of ILC3 vs. 15% ± 3% of ILC2; $p < 0.0001$) in all ATs, and this was also the case in EAT (Figure 2G). Exclusion of a patient with CAD did not significantly change the results (Figure S3).

Remarkably, a higher percentage of ILC2 (15% ± 2.7%) was observed in EAT than in thSAT (4% ± 1.7%) and VAT (4.4% ± 1.5%; $p = 0.0044$; Figure 2H). We also showed that almost 100% (97.9% ± 1.2%; $p < 0.0001$) of EAT-ILC2 expressed CD25 and/or CD69 activation markers compared with ILC1 (71.6% ± 1.2%; $p < 0.001$) and ILC3 (75% ± 7%; $p < 0.001$; Figure 2I). Taken together, these results showed that VAT contains more ILCs and NK cells than SAT and that the ILC1 subtype is the more represented in all fat depots. Moreover, EAT-ILC analysis showed that EAT contains more ILC2 compared with other ATs and that nearly all of the EAT-ILC2 expresses activation markers.

EAT gene phenotyping confirms upregulation of Th2 cells and browning genes compared with other ATs

BUB1B, IL-5, transcription factor 21 (TCF21), and IL-33 gene expression evaluated by qPCR was upregulated in EAT compared with SAT, with a high significance for the alarmin cytokine IL-33 ($p < 0.0001$ for ANOVA; Figure 3). Additionally, TBX20, MELK, and UHRF1 genes were found to be significantly upregulated in EAT compared with VAT (all $p < 0.05$; Figure 3). According to the pan-genomic study, we found upregulation of UCP-1 and alkaline phosphatase, biomineralization associated (ALPL) genes in EAT compared with VAT, abSAT, and thSAT ($p = 0.003$ and $p = 0.0062$ for ANOVA, respectively) and TNFRSF9 gene in EAT compared with thSAT ($p = 0.0075$ for ANOVA; Figure 4). FABP4 and CCAAT enhancer binding protein α (C/EBPα) genes were significantly downregulated in EAT versus abSAT and thSAT ($p < 0.0001$ and $p = 0.0003$ for ANOVA, respectively; Figure 4). Interestingly, we evidenced a positive correlation between the number of ILC1 per gram of AT and TNFRSF9 ($r = 0.55$; $p = 0.036$) and between the number of ILC2 per gram of AT and UCP-1 ($r = 0.64$; $p = 0.028$), TNFRSF9 ($r = 0.69$; $p = 0.006$), and ALPL ($r = 0.53$; $p = 0.017$). We also found a positive correlation between IL-13 gene expression and ILC1 and ILC2 per gram of AT ($r = 0.58$; $p = 0.008$ and $r = 0.55$; $p = 0.013$, respectively; Table 2).

DISCUSSION

This study is the first, to our knowledge, to describe individual immune cell populations and identify ILCs in human EAT using multiparametric FC methods.

We observed an increase in T cells compared with B cells in all ATs and an increase in ILCs (ILC1 > ILC3 > ILC2) and NK cells in VAT versus SAT. In addition, we observed a specific enrichment of ILC2 in EAT compared with other ATs, and these ILC2 were found to be highly activated.

Immunometabolism has been emerging in these last years as a key regulator of AT homeostasis. Components of the innate immune system such as AT macrophages (ATMs), dendritic cells, NK cells, and ILCs dominate the resident leukocyte population in AT. In 2003, Mazurek et al. provided the first evidence of this meta-inflammation in EAT and showed that $CD3^+$T cells, $CD68^+$ macrophages, and $tryptase^+$ mast cells infiltrate EAT compared with thSAT [21]. Recent studies with integrated bioinformatics analysis and immunohistochemistry have confirmed marked immune activation of IFN-γ^+ effector memory T cells in EAT of patients with heart failure and proinflammatory M1 polarization of ATMs with CAD [22]. However, the profile and microenvironment of ILCs within human EAT have never been studied before, to our knowledge, because of the difficulty in obtaining a sufficient amount of cardiac fat during open heart surgery [23]. Interestingly, recent developed drugs such as glucagon-like peptide-1 (GLP-1) receptor agonists can reduce EAT inflammation and

FIGURE 2 Distribution of adaptive and innate lymphoid cells (ILCs) in visceral adipose tissue (VAT) and subcutaneous AT (SAT). (A) Distribution of lymphocyte flow cytometry (FC) assay showing the number of T cells ($CD3^+$), $CD4^+$T cells ($CD3^+CD4^+$), $CD8^+$T cells ($CD3^+CD8^+$), and B cells ($CD19^+$) per gram of epicardial AT (EAT), thoracic subcutaneous AT (thSAT), VAT, and abdominal SAT (abSAT). (B) ILC gating. Helper ILCs are defined as $CD45^+Lin^-CD127^+$ cells. Among total ILCs, ILC1 are defined as $CD117^-CRTH2^-$ cells, ILC2 as $CD117^{+/-}CRTH2^+$, and ILC3 as $CD117^+CRTH2^-$. (C) Natural killer (NK) cells are defined as $CD3^-CD56/CD16^+$ cells among total lymphocytes. (D) Box plot representation of total ILC number in VAT (EAT and VAT) and SAT (thSAT and abSAT) per gram of tissue. (E) Distribution of ILC1, ILC2, and ILC3 subsets per gram of VAT or SAT. (F) Distribution of NK cells within EAT, thSAT, VAT, and abSAT. (G) Distribution of ILC subsets in EAT. (H) Quantification of ILC2 percentage per gram of tissue within all four ATs. (I) Percentage of $CD25^+$ and/or $CD69^+$ activated ILCs within EAT. Histogram data are represented as mean ± SEM and box plot data with the Tukey method. Comparison analyses between VAT and SAT were performed using *t* test or ANOVA; $n = 18$; $^*p < 0.05$; $^{**}p < 0.01$; $^{***}p < 0.001$. [Color figure can be viewed at wileyonlinelibrary.com]

1930739x, 0, Downloaded from https://onlinelibrary.wiley.com/doi/10.1002/oby.24023 by Cochrane France, Wiley Online Library on [16/05/2024]. See the Terms and Conditions (https://onlinelibrary.wiley.com/terms-and-conditions) on Wiley Online Library for rules of use; OA articles are governed by the applicable Creative Commons License

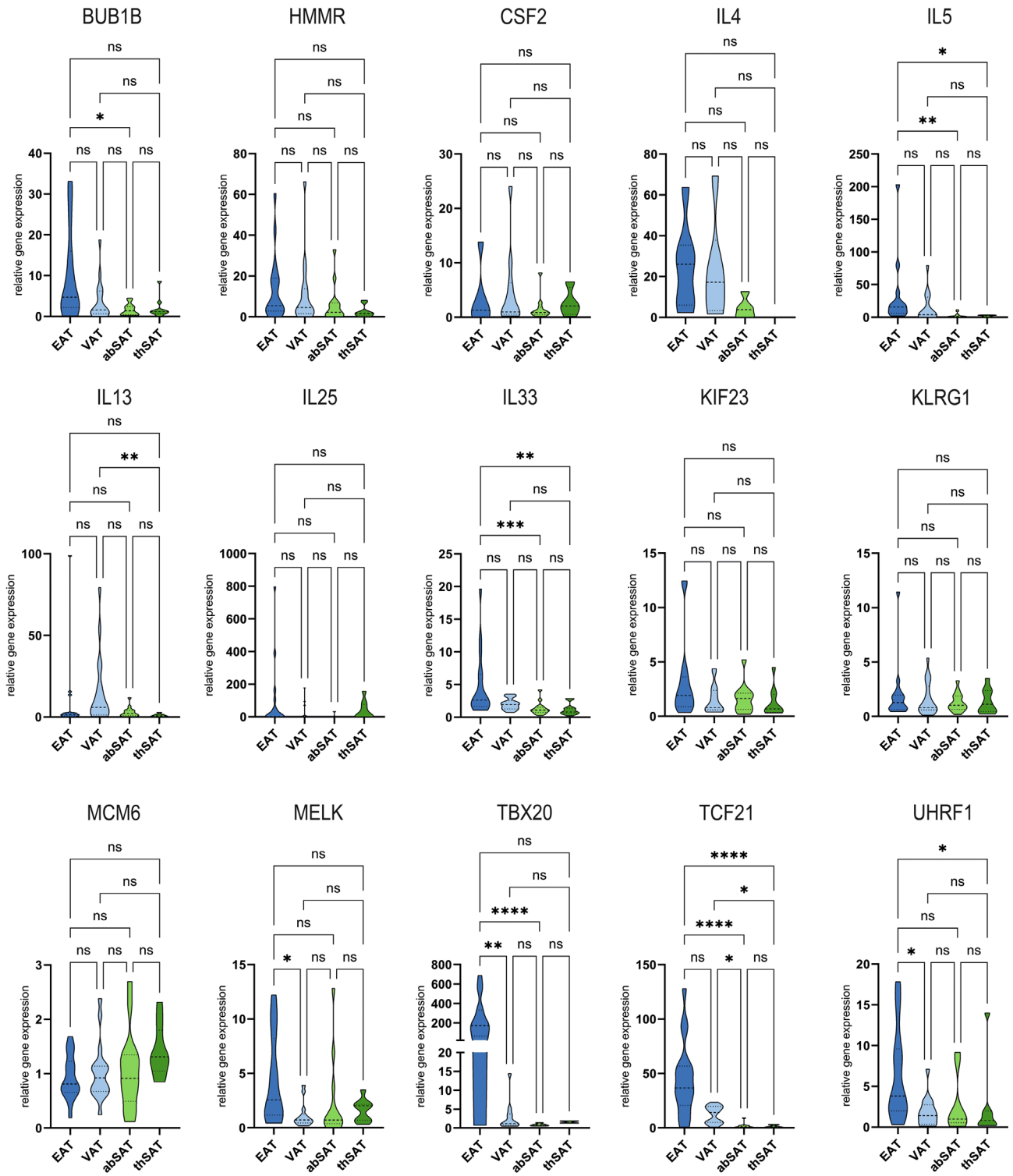

FIGURE 3 Comparative gene expression analysis of Th2 cell genes in the INTERFACE prospective study between epicardial adipose tissue (EAT), visceral AT (VAT), abdominal subcutaneous AT (abSAT), and thoracic SAT (thSAT). Violin plot data are represented as median ± IQR. Comparison analyses among ATs were performed using the Kruskall–Wallis test; $n = 18$; *$p < 0.05$; **$p < 0.01$; ***$p < 0.001$; ****$p < 0.0001$. IL-9 and SHOX2 data are not presented because Ct were >45. ns, not significant. [Color figure can be viewed at wileyonlinelibrary.com]

increase free fatty acid oxidation as fuel for the myocardium and induce fat browning; this GLP-1R-dependent browning effect on EAT could lead to improved myocardial insulin sensitivity and metabolism [24]. GLP-1, glucose-dependent insulinotropic polypeptide, and glucagon receptors are similarly present at mRNA and protein levels in human EAT, particularly in crown-like structures and,

1930739x, 0, Downloaded from https://onlinelibrary.wiley.com/doi/10.1002/oby.24023 by Cochrane France, Wiley Online Library on [16/05/2024]. See the Terms and Conditions (https://onlinelibrary.wiley.com/terms-and-conditions) on Wiley Online Library for rules of use; OA articles are governed by the applicable Creative Commons License

Obesity A Research Journal THE OBESITY SOCIETY WILEY

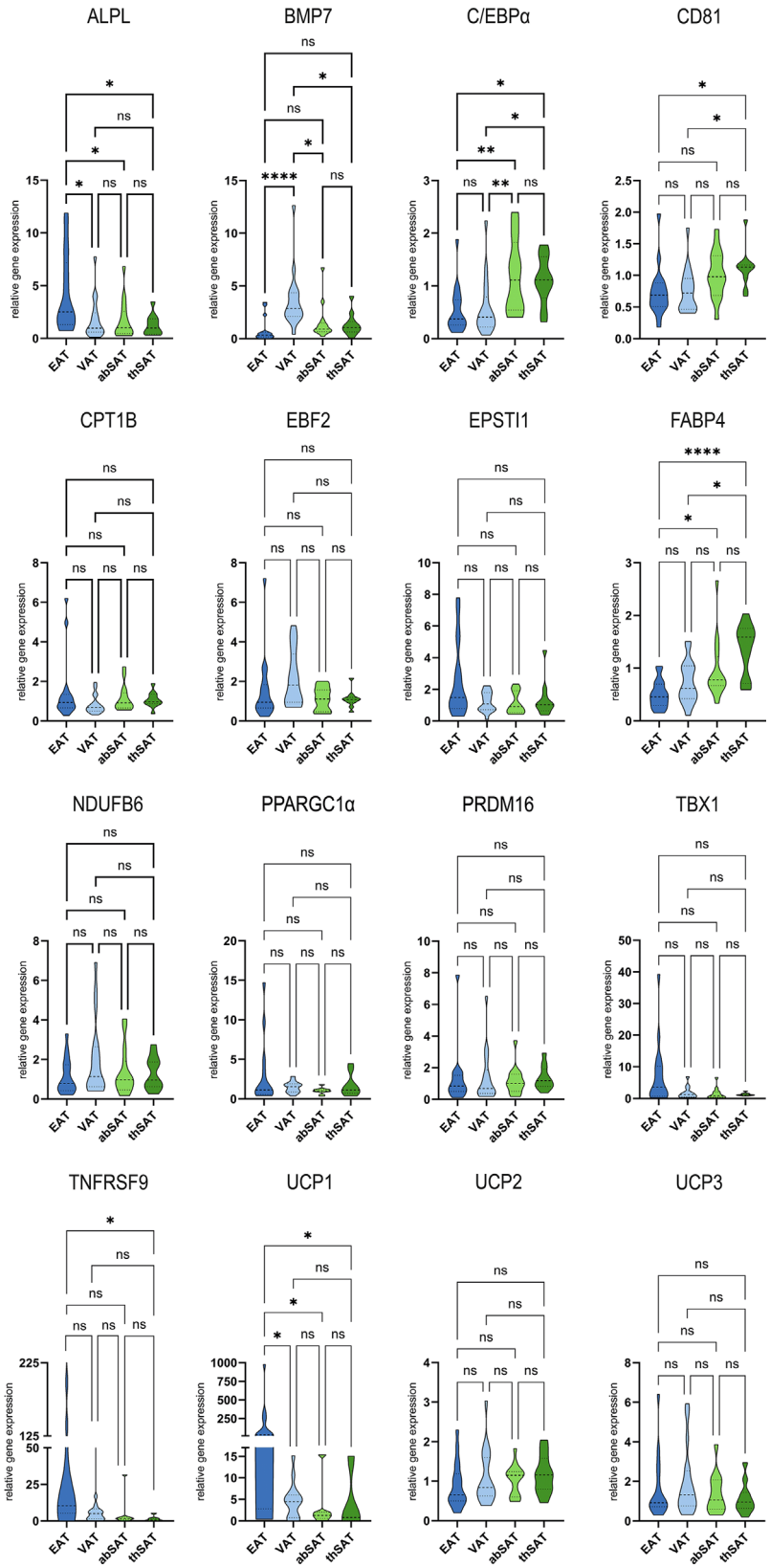

FIGURE 4 Comparative gene expression analysis of browning genes in the INTERFACE prospective study between epicardial adipose tissue (EAT), visceral AT (VAT), abdominal subcutaneous AT (abSAT), and thoracic SAT (thSAT). Violin plot data are represented as median ± IQR. Comparison analyses among ATs were performed using the Kruskall–Wallis test; $n = 18$; *$p < 0.05$; **$p < 0.01$; ****$p < 0.0001$. TMEM26, NRF1, and SLC2A4 data are not presented because Ct were >45. ns, not significant. [Color figure can be viewed at wileyonlinelibrary.com]

1930739x, 0, Downloaded from https://onlinelibrary.wiley.com/doi/10.1002/oby.24023 by Cochrane France, Wiley Online Library on [16/05/2024]. See the Terms and Conditions (https://onlinelibrary.wiley.com/terms-and-conditions) on Wiley Online Library for rules of use; OA articles are governed by the applicable Creative Commons License

TABLE 2 Correlation between relative browning or Th2 cell gene expression and ILC1, ILC2, or ILC3 per gram of all ATs.

		ILC1		ILC2		ILC3	
Pathways	**Gene**	***r***	***p* value**	***r***	***p* value**	***r***	***p* value**
Browning	ALPL	0.35	0.128	**0.53**	**0.017**	0.03	0.890
	BMP7	0.34	0.165	0.06	0.799	0.04	0.879
	CD81	**−0.54**	**0.015**	−0.35	0.125	**−0.54**	**0.015**
	C/EBPα	**−0.55**	**0.011**	−0.31	0.181	−0.35	0.135
	CIDEA	−0.42	0.068	−0.32	0.173	−0.41	0.071
	CPT1B	**−0.52**	**0.020**	−0.34	0.147	−0.40	0.083
	EBF2	−0.16	0.490	−0.20	0.403	−0.33	0.151
	EPSTI1	0.37	0.104	0.35	0.134	0.00	0.987
	FABP4	**−0.59**	**0.006**	**−0.47**	**0.037**	**−0.67**	**0.001**
	NDUFB6	−0.25	0.289	−0.11	0.654	−0.44	0.053
	PPARGC1A	0.18	0.447	0.12	0.627	0.04	0.862
	PPARγ	**−0.48**	**0.032**	−0.28	0.239	−0.32	0.172
	PRDM16	−0.29	0.212	0.02	0.937	−0.25	0.286
	SIRT5	−0.43	0.058	−0.27	0.246	**−0.65**	**0.002**
	SLC2A4	−0.34	0.140	−0.18	0.455	−0.36	0.121
	TBX1	−0.16	0.519	0.11	0.668	−0.33	0.169
	TIMM23	0.03	0.915	0.23	0.332	**−0.45**	**0.048**
	TNFRSF9	**0.55**	**0.036**	**0.69**	**0.006**	0.21	0.452
	UCP-1	0.22	0.499	**0.64**	**0.028**	0.09	0.783
	UCP-2	−0.05	0.850	−0.02	0.935	−0.17	0.487
	UCP-3	0.07	0.772	0.03	0.895	−0.04	0.865
Th2 cell	BUB1B	0.21	0.406	0.25	0.315	0.28	0.265
	CSF2	0.17	0.678	0.35	0.350	0.25	0.521
	HMMR	**0.51**	**0.023**	**0.53**	**0.015**	**0.47**	**0.035**
	IL-4	0.31	0.564	0.20	0.714	−0.03	>0.999
	IL-5	0.21	0.430	0.32	0.220	0.23	0.388
	IL-13	**0.58**	**0.008**	**0.55**	**0.013**	0.29	0.215
	IL-25	−0.12	0.617	0.02	0.920	0.03	0.915
	IL-33	0.32	0.171	0.32	0.173	0.21	0.375
	KIF23	0.34	0.171	0.35	0.152	0.45	0.062
	KLRG1	−0.06	0.796	0.05	0.830	−0.14	0.548
	MCM6	0.06	0.796	−0.05	0.830	0.14	0.548
	MELK	0.00	0.987	0.08	0.760	−0.10	0.680
	TBX20	−0.20	0.543	0.16	0.619	−0.14	0.671
	TCF21	0.46	0.054	**0.63**	**0.006**	0.34	0.172
	UHRF1	0.45	0.094	0.51	0.053	0.38	0.161

Note: Correlation with Spearman nonparametric test; bold values denote statistical significance ($p < 0.05$).
Abbreviations: AT, adipose tissue; ILC, innate lymphoid cell.

partially, in adipocytes [25]. Whether other adipose resident immune cells express these receptors remains unknown.

Our transcriptomic study confirms that EAT was specifically enriched in transcripts from the Th2 cell signaling pathway and also provides evidence that these pathways are correlated with browning genes [23, 26]. This is interesting because recent research has indicated that ILC2 effector function is responsible for enhanced AT browning and an anti-inflammatory immune profile [11, 13]. Accordingly, EAT had more ILC2 than other ATs, and these cells displayed markers of activation (CD25 and CD69), highlighting their potential role in thermogenic activity, which we and others have previously evidenced [8, 9]. Moreover, gene expression phenotyping confirmed upregulation of specific ILC2 alarmin cytokines such as IL-33 in EAT and a positive correlation between IL-13 gene expression and ILC2

1930739x, 0, Downloaded from https://onlinelibrary.wiley.com/doi/10.1002/oby.24023 by Cochrane France, Wiley Online Library on [16/05/2024]. See the Terms and Conditions (https://onlinelibrary.wiley.com/terms-and-conditions) on Wiley Online Library for rules of use; OA articles are governed by the applicable Creative Commons License

quantification in all ATs. However, further functional studies are warranted to identify which mediators trigger ILC2 activation and whether ILC2 may be causative in the regulation of EAT thermogenic activity [12]. Additionally, both EAT mitochondrial function and brown AT-like thermogenic activity decrease with advanced CAD and aging, and low mitochondrial respiration in EAT was associated with CAD severity [27].

On the other hand, ILC1 were the most abundant ILC subtype in all ATs. Co-culture and adoptive transfer studies have shown that ILC1 from human AT promote adipose fibrogenesis by activating transforming growth factor β 1 signaling and $CD11c^{+}$ macrophage activation in obesity [28].

In mice, removal of pericardial AT, which contained a high density of lymphoid clusters, prevented adaptive immune cell response triggered by coronary artery ligation and ischemic cardiac injury, limited fibrosis, and decreased ejection fraction [29]. Recent studies have shown that ILC1 and ILC2 play opposite roles in atherosclerosis pathogenesis. Increased circulating ILC1 have been found in patients with acute ST-segment elevation myocardial [30] or cerebral infarction [31] and correlated with higher oxidized low-density lipoprotein levels. By contrast, ILC2 are decreased in patients with myocardial [30] or cerebral [31] infarcts and in obese mice. Furthermore, genetic ablation of ILC2 favors atherosclerosis development [32], whereas their expansion through direct adoptive transfer or via administration of IL-2 [33] and IL-25 [34] is atheroprotective. Whether ILC1 are implicated in the proinflammatory profile of EAT in patients with CAD has not been elucidated.

Under homeostatic lean conditions, ILC2, eosinophils, or anti-inflammatory ATMs are present within AT [35]. In obesity, the composition of inflammatory cells switches to an accumulation of ILC1, proinflammatory ATMs, $CD8^{+}$T cells, or Th1 and Th17 cells within SAT [36, 37]. Adoptive transfer of adipose ILC1 from obese mice exaggerated their accumulation in recipient mice and amplified glucose intolerance [28]. ILC1-mediated IFN-γ production enhanced macrophages to promote a dysregulated proinflammatory microenvironment, favoring insulin resistance [14].

ILC2 have been shown to be resident in white AT and decreased in obesity [11, 35]. Indeed, when stimulated via administration of alarmin IL-25 or IL-33, ILC2 promote an anti-inflammatory type 2 environment via eosinophil recruitment and alternatively activated macrophage induction [11]. Mice treated with ILC2 adoptive transfer or via administration of IL-33 had an increased number of UCP-1 positive beige cells within white AT [11]. Furthermore, ILC2 can produce methionine-enkephalin peptides, which upregulate UCP-1 in adipocytes in vitro and promote the beiging of AT in vivo [11]. Consistent with this, qPCR analysis confirmed upregulation of UCP-1, ALPL, and TNFRSF9 gene expression in EAT versus other ATs, as well as a positive correlation among expression of these genes and ILC2 quantification in all ATs. Thus, better identifying the imbalance between ILCs in AT and in EAT could help to better target its immunometabolic profile.

Various methods to manipulate ILCs have been developed recently such as the inhibition of ILC migration and function [38–40], microbiome manipulation [41], glucocorticoid [42], or even β_2 adrenergic receptor agonists [43]. Others such as adoptive transfer, anticytokine antibodies, or even immune checkpoint modulation have been also used to fight against atherosclerosis, obesity, or T2D in humans and/or mice. Interestingly, glucocorticoid-induced TNF receptor (GITR) engagement on activated ILC2 not only stimulates secretion of ILC2 effector cytokines but also prevents ILC2 apoptosis. A GITR agonist reversed established glucose intolerance by inducing adipocyte beiging via IL-13 secretion [44]. Thus, therapeutic activation of the IL-33/GITR/ILC2 beiging pathway could represent an interesting target to reduce the EAT inflammatory phenotype [44].

Given their recent identification, and apart from the numerous studies that aimed at understanding their role in obesity and browning, ILCs have never been studied in EAT, to our knowledge. Their role in the pathophysiology of epicardial fat and, extensively, in cardiovascular disease remains to be understood.

Our study has several limitations. This study provides correlative data, and no causal conclusions can be drawn regarding the presence of ILC2 and the beiging profile of EAT, which merit further investigation. The small sample size of patients did not allow us to analyze the impact of obesity, T2D, or CAD on the immune profile of EAT, and we probably lacked statistical power to clearly differentiate EAT from VAT immunophenotype; however, we faced many refusals of organ donation and sampling for experimental studies from deceased patients' families. However, a recent study has shown that obesity and T2D significantly increase the inflammatory profile and the expression of immune mediators in EAT [45]. Finally, due to the small sample size, we likely lack sufficient power to identify objective differences in the different ILC subtypes and had to pull data regarding VAT and SAT.

CONCLUSION

In this study, we compared individual immune cell populations of various ATs and reported that ILC2 are highly represented in EAT. This might suggest that these cells could have a role in its beiging profile.O

AUTHOR CONTRIBUTIONS

Conceptualization, Bénédicte Gaborit, Anne Dutour, and Frédéric Vély; methodology, Frédéric Vély, Elisa Doukbi, Patricia Ancel, Shaista Ahmed, Victoria Castejon, Christelle Piperoglou, and Mikael Ebbo; analysis, Elisa Doukbi, Astrid Soghomonian, Shaista Ahmed, Victoria Castejon, Christelle Piperoglou, and Frédéric Vély; data interpretation, Elisa Doukbi, Bénédicte Gaborit, Anne Dutour, and Patricia Ancel; sampling collection, Vlad Gariboldi, Marien Lenoir, Eric Lechevallier, Bastien Gondran-Tellier, and Romain Boissier; literature search, Elisa Doukbi and Bénédicte Gaborit; writing (original draft preparation), Elisa Doukbi and Bénédicte Gaborit; writing (review and editing), Anne Dutour, Frédéric Vély, Romain Boissier, and Marien Lenoir; supervision, Bénédicte Gaborit, Anne Dutour, and Frédéric Vély; project administration, Patricia Ancel; and funding acquisition, Bénédicte Gaborit. All authors have read and agreed to the published version of the manuscript.

1930739x, 0, Downloaded from https://onlinelibrary.wiley.com/doi/10.1002/oby.24023 by Cochrane France, Wiley Online Library on [16/05/2024]. See the Terms and Conditions (https://onlinelibrary.wiley.com/terms-and-conditions) on Wiley Online Library for rules of use; OA articles are governed by the applicable Creative Commons License

ACKNOWLEDGMENTS

We want to thank all of the Immunopole team for their technical support in multiparametric FC, as well as Elise Dalmas from Immediab Team, Paris, for her help in Th2 cell pathway genes listing. We are also very grateful to all of the organ donation coordination teams from the Marseille and Toulon regions for their help in collecting samples and checking family agreement, as well as all of the patients' families for their help in scientific research advances.

FUNDING INFORMATION

This work received support from the French government under the France 2030 investment plan as part of the Aix-Marseille University Excellence Initiative—A*MIDEX (AMX-21-PEP-026). The project was also carried out with the support of the Fondation de l'Avenir (Paris, France, 2022, AP-RM-22-017).

CONFLICT OF INTEREST STATEMENT

The authors declared no conflict of interest.

DATA AVAILABILITY STATEMENT

The datasets used and/or analyzed during the current study are available from the corresponding author on reasonable request.

ORCID

Elisa Doukbi https://orcid.org/0009-0007-2634-0352
Anne Dutour https://orcid.org/0000-0002-5844-5884
Shaista Ahmed https://orcid.org/0000-0003-4695-4718
Marien Lenoir https://orcid.org/0000-0003-0272-5753
Bastien Gondran-Tellier https://orcid.org/0000-0002-7839-9504
Romain Boissier https://orcid.org/0000-0001-6428-0273
Mikael Ebbo https://orcid.org/0000-0002-1179-8113
Frédéric Vély https://orcid.org/0000-0002-1682-0949
Bénédicte Gaborit https://orcid.org/0000-0002-4180-158X

REFERENCES

1. Baker AR, da Silva NF, Quinn DW, et al. Human epicardial adipose tissue expresses a pathogenic profile of adipocytokines in patients with cardiovascular disease. *Cardiovasc Diabetol*. 2006;5:1.
2. Gruzdeva O, Uchasova E, Dyleva Y, et al. Adipocytes directly affect coronary artery disease pathogenesis via induction of adipokine and cytokine imbalances. *Front Immunol*. 2019;10:2163.
3. Gaborit B, Sengenes C, Ancel P, Jacquier A, Dutour A. Role of epicardial adipose tissue in health and disease: a matter of fat? *Compr Physiol*. 2017;7:1051-1082.
4. Gaborit B, Abdesselam I, Dutour A. Epicardial fat: more than just an "epi" phenomenon? *Horm Metab Res*. 2013;45:991-1001.
5. Iacobellis G. Epicardial adipose tissue in contemporary cardiology. *Nat Rev Cardiol*. 2022;19:593-606.
6. Venteclef N, Guglielmi V, Balse E, et al. Human epicardial adipose tissue induces fibrosis of the atrial myocardium through the secretion of adipo-fibrokines. *Eur Heart J*. 2015;36:795-805a.
7. Camarena V, Sant D, Mohseni M, et al. Novel atherogenic pathways from the differential transcriptome analysis of diabetic epicardial adipose tissue. *Nutr Metab Cardiovasc Dis*. 2017;27:739-750.
8. Sacks HS, Fain JN, Bahouth SW, et al. Adult epicardial fat exhibits beige features. *J Clin Endocrinol Metab*. 2013;98:E1448-E1455.
9. Gaborit B, Venteclef N, Ancel P, et al. Human epicardial adipose tissue has a specific transcriptomic signature depending on its anatomical peri-atrial, peri-ventricular, or peri-coronary location. *Cardiovasc Res*. 2015;108:62-73.
10. Barchuk M, Dutour A, Ancel P, et al. Untargeted lipidomics reveals a specific enrichment in plasmalogens in epicardial adipose tissue and a specific signature in coronary artery disease. *Arterioscler Thromb Vasc Biol*. 2020;40:986-1000.
11. Brestoff JR, Kim BS, Saenz SA, et al. Group 2 innate lymphoid cells promote beiging of white adipose tissue and limit obesity. *Nature*. 2015;519:242-246.
12. Doukbi E, Soghomonian A, Sengenès C, et al. Browning epicardial adipose tissue: friend or foe? *Cells*. 2022;11:991.
13. Lee M-W, Odegaard JI, Mukundan L, et al. Activated type 2 innate lymphoid cells regulate beige fat biogenesis. *Cell*. 2015;160:74-87.
14. O'Sullivan TE, Rapp M, Fan X, et al. Adipose-resident group 1 innate lymphoid cells promote obesity-associated insulin resistance. *Immunity*. 2016;45:428-441.
15. Carpentier AC, Blondin DP, Haman F, Richard D. Brown adipose tissue—a translational perspective. *Endocr Rev*. 2023;44:143-192.
16. Deslex S, Negrel R, Vannier C, Etienne J, Ailhaud G. Differentiation of human adipocyte precursors in a chemically defined serum-free medium. *Int J Obes (Lond)*. 1987;11:19-27.
17. Hauner H, Entenmann G, Wabitsch M, et al. Promoting effect of glucocorticoids on the differentiation of human adipocyte precursor cells cultured in a chemically defined medium. *J Clin Invest*. 1989;84:1663-1670.
18. Carvelli J, Piperoglou C, Bourenne J, et al. Imbalance of circulating innate lymphoid cell subpopulations in patients with septic shock. *Front Immunol*. 2019;10:2179.
19. Vély F, Barlogis V, Vallentin B, et al. Evidence of innate lymphoid cell redundancy in humans. *Nat Immunol*. 2016;17:1291-1299.
20. Chechi K, Gelinas Y, Mathieu P, Deshaies Y, Richard D. Validation of reference genes for the relative quantification of gene expression in human epicardial adipose tissue. *PloS One*. 2012;7:e32265.
21. Mazurek T, Zhang L, Zalewski A, et al. Human epicardial adipose tissue is a source of inflammatory mediators. *Circulation*. 2003;108:2460-2466.
22. Hirata Y, Tabata M, Kurobe H, et al. Coronary atherosclerosis is associated with macrophage polarization in epicardial adipose tissue. *J Am Coll Cardiol*. 2011;58:248-255.
23. Klein M, Varga I. Microenvironment of immune cells within the visceral adipose tissue sensu lato vs. epicardial adipose tissue: what do we know? *Inflammation*. 2018;41:1142-1156.
24. Beiroa D, Imbernon M, Gallego R, et al. GLP-1 agonism stimulates brown adipose tissue thermogenesis and browning through hypothalamic AMPK. *Diabetes*. 2014;63:3346-3358.
25. Malavazos AE, Iacobellis G, Dozio E, et al. Human epicardial adipose tissue expresses glucose-dependent insulinotropic polypeptide, glucagon, and glucagon-like peptide-1 receptors as potential targets of pleiotropic therapies. *Eur J Prev Cardiol*. 2023;30:680-693.
26. Chechi K, Vijay J, Voisine P, et al. UCP1 expression–associated gene signatures of human epicardial adipose tissue. *JCI Insight*. 2019;4:e123618.
27. Nakajima T, Yokota T, Shingu Y, et al. Impaired mitochondrial oxidative phosphorylation capacity in epicardial adipose tissue is associated with decreased concentration of adiponectin and severity of coronary atherosclerosis. *Sci Rep*. 2019;9:3535.
28. Wang H, Shen L, Sun X, et al. Adipose group 1 innate lymphoid cells promote adipose tissue fibrosis and diabetes in obesity. *Nat Commun*. 2019;10:3254.
29. Horckmans M, Bianchini M, Santovito D, et al. Pericardial adipose tissue regulates granulopoiesis, fibrosis, and cardiac function after myocardial infarction. *Circulation*. 2018;137:948-960.

1930739x, 0, Downloaded from https://onlinelibrary.wiley.com/doi/10.1002/oby.24023 by Cochrane France, Wiley Online Library on [16/05/2024]. See the Terms and Conditions (https://onlinelibrary.wiley.com/terms-and-conditions) on Wiley Online Library for rules of use; OA articles are governed by the applicable Creative Commons License

30. Li J, Wu J, Zhang M, Zheng Y. Dynamic changes of innate lymphoid cells in acute ST-segment elevation myocardial infarction and its association with clinical outcomes. *Sci Rep*. 2020;10:5099.
31. Li Q, Liu M, Fu R, et al. Alteration of circulating innate lymphoid cells in patients with atherosclerotic cerebral infarction. *Am J Transl Res*. 2018;10:4322-4330.
32. Newland SA, Mohanta S, Clément M, et al. Type-2 innate lymphoid cells control the development of atherosclerosis in mice. *Nat Commun*. 2017;8:15781.
33. Engelbertsen D, Foks AC, Alberts-Grill N, et al. Expansion of CD25+ innate lymphoid cells reduces atherosclerosis. *Arterioscler Thromb Vasc Biol*. 2015;35:2526-2535.
34. Mantani PT, Dunér P, Bengtsson E, et al. IL-25 inhibits atherosclerosis development in apolipoprotein E deficient mice. *PloS One*. 2015;10:e0117255.
35. Molofsky AB, Nussbaum JC, Liang H-E, et al. Innate lymphoid type 2 cells sustain visceral adipose tissue eosinophils and alternatively activated macrophages. *J Exp Med*. 2013;210:535-549.
36. Yang H, Youm Y-H, Vandanmagsar B, et al. Obesity increases the production of proinflammatory mediators from adipose tissue T cells and compromises TCR repertoire diversity: implications for systemic inflammation and insulin resistance. *J Immunol*. 2010;185:1836-1845.
37. Schwartz C, Schmidt V, Deinzer A, et al. Innate PD-L1 limits T cell–mediated adipose tissue inflammation and ameliorates diet-induced obesity. *Sci Transl Med*. 2022;14:eabj6879.
38. Sonnenberg GF, Artis D. Innate lymphoid cells in the initiation, regulation and resolution of inflammation. *Nat Med*. 2015;21:698-708.
39. Eken A, Yetkin MF, Vural A, et al. Fingolimod alters tissue distribution and cytokine production of human and murine innate lymphoid cells. *Front Immunol*. 2019;10:217.
40. Filgotinib in the Induction and Maintenance of Remission in Subjects With Moderately to Severely Active Crohn's Disease (DIVERSITY1). ClinicalTrials.gov identifier NCT02914561. Published December 18, 2023. https://classic.clinicaltrials.gov/ct2/show/NCT02914561
41. Enterome. https://www.enterome.com/
42. Walford HH, Lund SJ, Baum RE, et al. Increased ILC2s in the eosinophilic nasal polyp endotype are associated with corticosteroid responsiveness. *Clin Immunol*. 2014;155:126-135.
43. Moriyama S, Brestoff JR, Flamar A-L, et al. β2-adrenergic receptor-mediated negative regulation of group 2 innate lymphoid cell responses. *Science*. 2018;359:1056-1061.
44. Galle-Treger L, Sankaranarayanan I, Hurrell BP, et al. Costimulation of type-2 innate lymphoid cells by GITR promotes effector function and ameliorates type 2 diabetes. *Nat Commun*. 2019;10:713.
45. Vyas V, Blythe H, Wood EG, et al. Obesity and diabetes are major risk factors for epicardial adipose tissue inflammation. *JCI Insight*. 2021;6:e145495.

SUPPORTING INFORMATION

Additional supporting information can be found online in the Supporting Information section at the end of this article.

How to cite this article: Doukbi E, Ancel P, Dutour A, et al. Human epicardial fat has a beige profile and contains higher type 2 innate lymphoid cells than subcutaneous fat. *Obesity (Silver Spring)*. 2024;1-13. doi:10.1002/oby.24023

1930739x, 0, Downloaded from https://onlinelibrary.wiley.com/doi/10.1002/oby.24023 by Cochrane France, Wiley Online Library on [16/05/2024]. See the Terms and Conditions (https://onlinelibrary.wiley.com/terms-and-conditions) on Wiley Online Library for rules of use; OA articles are governed by the applicable Creative Commons License